Available online at www.sciencedirect.com
SCIENCE DIRECT
Polymer Degradation and Stability 84 (2004) 545–553
Polymer Degradation and Stability
www.elsevier.com/locate/polydegstab

Viscoelastic properties and thermal degradation kinetics of silica/PMMA nanocomposites

Yu-Hsiang Hu[a], Chuh-Yung Chen[a,*], Cheng-Chien Wang[b]

[a]Department of Chemical Engineering, National Cheng-Kung University, Tainan 70101, Taiwan
[b]Department of Chemical Engineering, Southern Taiwan University of Technology, Tainan 717, Taiwan

Received 23 September 2003; received in revised form 9 February 2004; accepted 22 February 2004

Abstract

PMMA-silica nanocomposites were prepared using a bulk polymerization technique. Three organic silica groups, two modified with methyl groups and the third an octane, made these inorganic silica particles more hydrophobic. These silica/PMMA nanocomposites exhibited higher storage and loss moduli than those of pristine PMMA. The T_g of these composites increased with the silica content. The thermal characteristics of these composites were also enhanced by incorporating silica into the PMMA matrix. The degradation temperature at 10% weight loss was approximately 30 °C higher than that of pristine PMMA, depending upon the silica content. The rate of weight loss at 220 °C for 2 h was also markedly reduced in the presence of these modified silicas. The results might be attributed to "trapping effect". The activation energies for these silica/PMMA nanocomposites were enhanced according to Flynn, Ozawa–Flynn, and Kissinger methods.

Keywords: PMMA; TGA; Activation energy; Silica

1. Introduction

Recently, the potential of using inorganic minerals as fillers in polymeric composites has become appreciated in areas of commercial and scientific application, and many investigations have been published [1–7]. The mechanical and thermal properties of inorganic/organic nanocomposites are expected to be considerably improved when the largest possible inorganic surface area is presented to the matrix. To achieve this improvement, the fillers must be fully dispersed throughout, and connected to the matrix using an appropriately modified intermediary to increase the hydrophobicity of the inorganic composites [8]. Silica particles, however, are difficult to disperse in organic solvent without surfactant because they tend to form large aggregations.

This work concerns the problem of silica particle dispersion and demonstrates a route to prevent the aggregation of silica by modifying silica surface. These modified silica particles disperse well among various monomers to form inorganic/polymer nanocomposites. Moreover, organically modified silica makes inorganic components more hydrophobic, causing them to disperse effectively throughout organic solvent or polymer matrices. Therefore, inorganic/organic nanocomposites without aggregated inorganic components in the polymer phases are obtained. Briefly, the organic modification of inorganic components is the most important process prior to the preparation of inorganic/polymer nanocomposites.

This study examines the bulk polymerization of methyl methacrylate (MMA). AEROSIL® R805, R812 and R972 were used as the three modified silicas, which were treated with amorphous silica, as indicated in Fig. 1. Numerous inorganic/PMMA nanocomposites have recently been investigated [9–15], and found to exhibit some properties superior to those of pure PMMA. Silicas are commercially available and the effects

* Corresponding author. Tel.: +886-6-2757575-62643; fax: +886-6-2360464.
E-mail address: ccy7@ccmail.ncku.edu.tw (C.-Y. Chen).

0141-3910/$ - see front matter © 2004 Elsevier Ltd. All rights reserved.
doi:10.1016/j.polymdegradstab.2004.02.001

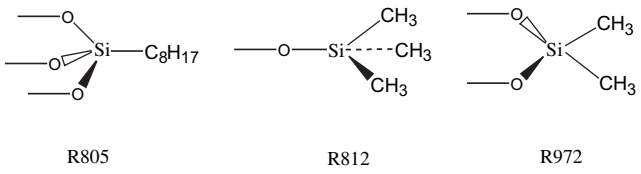

Fig. 1. The three modified silica structures R805, R812, and R972.

between a modified silica surface and the PMMA matrix have been studied to improve their utility, related to mechanical properties, hardness and surface abrasion.

Reliable kinetic parameters for the thermal degradation of silica/PMMA nanocomposites are determined. Even if the degradation has been extensively studied [16–24], there are lots of investigations for the thermal degradation of inorganic/PMMA composites. Most researchers have examined layered silicate composites or the use of in situ sol–gel processes to improve interactions to prepare silica/PMMA nanocomposites. The relationships between the properties of the polymer and the content of modifying silica are interesting. This paper describes a simple approach that involves adding modified silica to MMA solution to generate the silica/PMMA composites, and considers the relationships between the modified silica surface and the PMMA matrix, and mechanical and thermal behaviors.

2. Experimental

2.1. Materials

Methyl methacrylate (MMA) was distillated twice before being used. Three species of modified silica particles, AEROSIL® R805, R812 and R972, were used as received. Fig. 2 indicates that methyl ($-CH_3$) and ethylene ($-CH_2-$) groups (2862 cm^{-1}–2963 cm^{-1}) are present in the modified silica, but $-OH$ groups (3421 cm^{-1}) are present in the unmodified silica. FT-IR confirmed the presence of organics in the modified silica product and confirmed the integrity of the organic molecules. 2,2′-Azobisisobutyronitrile (AIBN) from Fluka was recrystallized twice from methanol before it was used as a radical initiator.

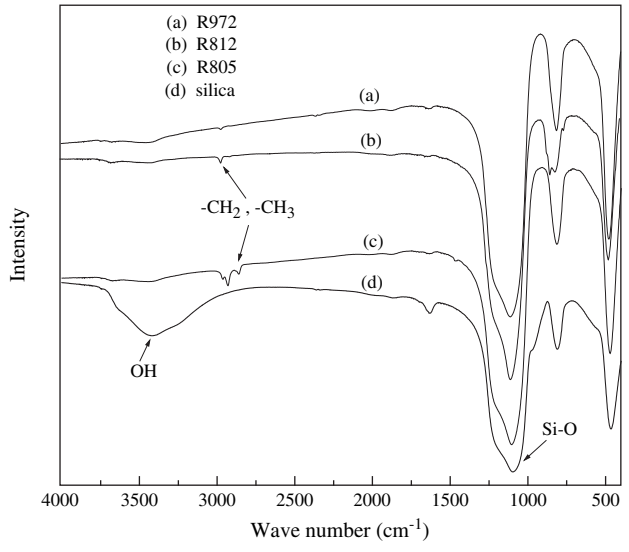

Fig. 2. The FT-IR spectra of silica- (a) R972, (b) R812, (c) R805, and (d) not modified silica.

2.2. Preparation of silica/PMMA composites

Before the silica/PMMA nanocomposites were prepared, the silica powder was well dispersed throughout the MMA monomer under sonification to yield various concentrations of silica/MMA solution. The different concentrations of silica/MMA solution (100 g) with 0.7 g AIBN were placed in a 200 ml beaker. This mixture was stirred at room temperature under flowing nitrogen, and then was warmed to 80 °C for 30 min for polymerization; it was cooled to room temperature to cast using 3 mm PVC packing. Finally, the mixture was polymerized at 55 °C for another 12 h in a water bath, and cured at 110 °C for an hour.

2.3. Characterization and measurement

Infrared spectroscopy, FT-IR, was conducted using a BIO-RAD FTS-40A + UMA500 spectrometer with KBr pellet at 4 cm^{-1} resolution. A dynamic mechanical analysis of the composites was performed using a Du-Pont 2980 Dynamic Mechanical Analyzer at a heating rate of 10 °C/min. The microstructures of the silica/PMMA nanocomposites were characterized using a Hitachi 4500 SEM at an acceleration voltage of 5K V. Thermogravimetry (TGA) was performed using a TA TGA-Q50 thermobalance. Samples of approximately 10–15 mg were heated at various heating rates under nitrogen purge (70 ml/min). Isothermal TGA was carried out by heating the sample to 220 °C for 2 h under nitrogen purge.

3. Results and discussion

3.1. Viscoelastic properties of modified silica/PMMA nanocomposites

Figs. 3 and 4 plot the storage modulus (E') and loss modulus (E'') of silica-R805/PMMA nanocomposites, obtained by DMA measurement. The storage modulus connects with the elastic modulus of the materials, and the loss modulus relates to the energy lost due to polymer chain movement. Below the glassy transition temperature, the silica/PMMA nanocomposites exhibit a high storage modulus. The storage moduli of the silica-R805/PMMA nanocomposites at about 40 °C are

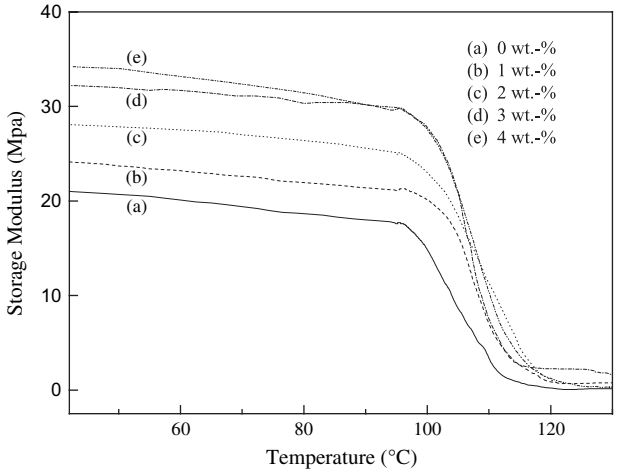

Fig. 3. Storage modulus, E', of the silica-R805/PMMA nanocomposites with various silica contents.

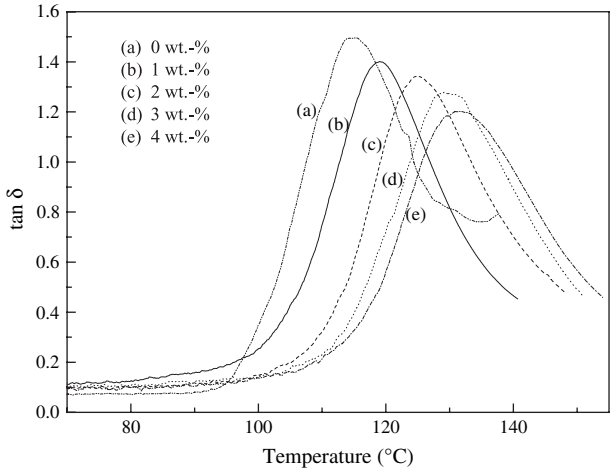

Fig. 5. tan δ of silica-R805/PMMA nanocomposites with various silica contents.

improved by introducing rigid silica particles. The stiffness associated with the modified silica particles dispersed well within the PMMA matrix causes the storage modulus to increase with silica content. The loss modulus of silica-R805/PMMA nanocomposites at around 50 °C also increases with the silica content because of the friction between the modified silica particles and the PMMA molecules when the silica particles are thoroughly dispersed in the PMMA matrix. The results reveal that the silica-R805 excellently reinforces the mechanical properties of pristine PMMA. The maximum E'' in Fig. 4 indicates that T_g of the silica-R805/PMMA nanocomposites increased with the silica content. The T_g of these silica/PMMA composites exceeds that of pure PMMA because the well-dispersed silica layers restrict the mobility of the PMMA chain and the modified silica surface is entangled with the PMMA molecules.

Fig. 5 plots the dependence of tan δ on temperature for silica-R805/PMMA nanocomposites. The loss factor tan δ is very sensitive to the structural transformation of the materials, and can be calculated from the ratio of the loss modulus to the storage modulus (E''/E'). Adding modified silica particles to the PMMA matrix shifts the tan δ peak values of these composites to the high-temperature region, implying an interaction between silica and the PMMA molecules. Increasing the silica content also broadens the tan δ peak, and lowers its intensity from 1.5 to 1.1. The breadth of the tan δ peak relates to the relaxation of the polymer chain. The adhesion between the modified surface of the silica particles and the PMMA molecules, and the constraints on the mobility of the polymer chains due to their being tethered to the inorganic particles widen the range of temperatures covered by the tan δ peak. Hence, the breadth of the tan δ peak increases with the silica content, and the height of the tan δ peak measures the energy-damping characteristics of a material. The silica particles are well dispersed in the PMMA matrix, so the rigid silica particles directly enhance the stiffness of the silica-R805/PMMA nanocomposites. The height of the tan δ peak thus declines as silica content increases.

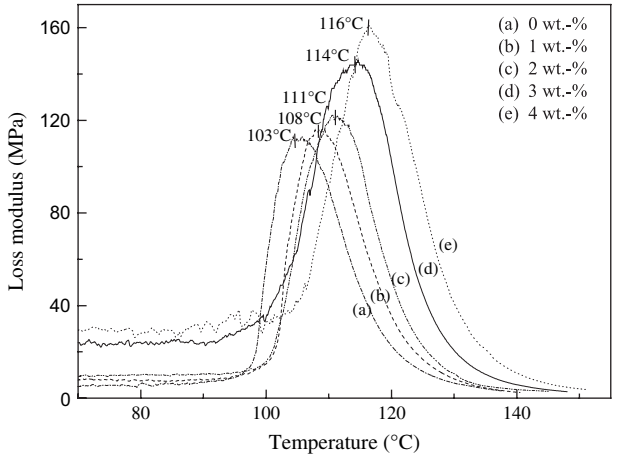

Fig. 4. Loss modulus, E'', of the silica-R805/PMMA nanocomposites with various silica contents.

Fig. 6 plots the relationship between the storage modulus of the variously modified silica/PMMA nanocomposites and the silica content. The storage modulus increased with the silica content for all modified silica/PMMA composites. Additionally, the moduli increased by about 30%, 40% and 56% for silica-R972/PMMA, silica-R812/PMMA and silica-R805/PMMA nanocomposites, respectively, at a silica loading of 4 wt%. The silica-R805/PMMA composite has higher storage modulus than silica-R812/PMMA and silica-R972/PMMA composites, perhaps because the silica-R805 particles can be more easily dispersed effectively in the PMMA matrix, causing stronger interactions than the other two modified silicas, increasing the elastic modulus of the materials.

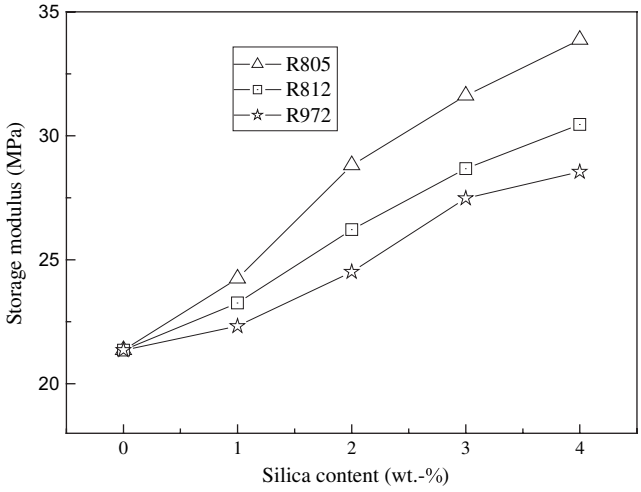

Fig. 6. The comparison of storage modulus of different silica/PMMA nanocomposites with various silica contents.

Fig. 7 reveals the maximum of the loss modulus of these modified silica/PMMA nanocomposites. All the loss moduli increased with the silica content. It can be observed that the loss modulus of the silica-R805/PMMA increases slightly with loading up to 2 wt%, and then rises rapidly as silica is added beyond 2 wt%. Unlike those of the other two composites, silica-R812/PMMA and silica-R972/PMMA, the loss modulus increases smoothly. The phenomena may be attributed to the increase in the friction between the modified silica-R805 surface group (octane) and the PMMA molecules with the silica-R805 content above 2 wt%, and the fact that the interactions between the other two methyl groups on the modified silica-R812 and -R972 are weaker, even as the silica content is increased to 4 wt%.

Fig. 8 plots the relationship between the glass transition temperature (T_g) of the differently modified

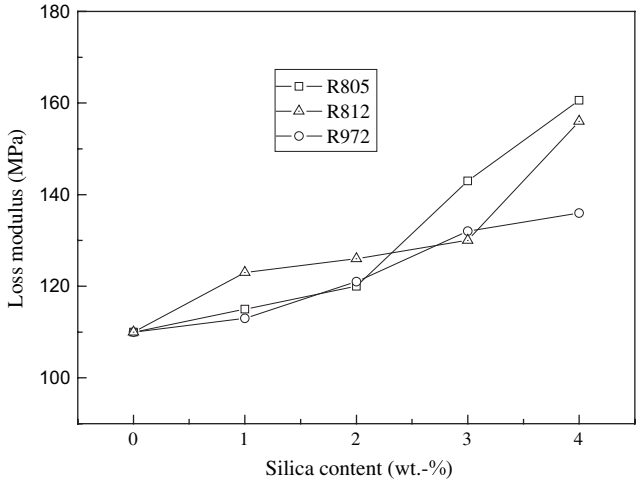

Fig. 7. The comparison of loss modulus of different silica/PMMA nanocomposites with various silica contents.

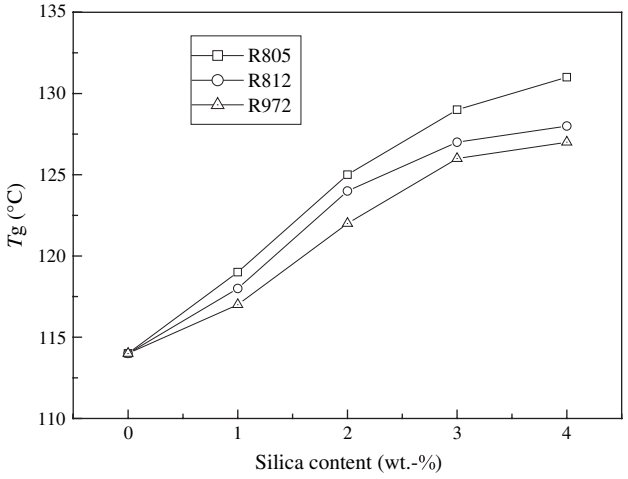

Fig. 8. The comparison of T_g for different silica/PMMA nanocomposites with various silica contents.

silica/PMMA nanocomposites and the silica content. All the T_g values of the modified silica/PMMA composites increased with the silica content. The T_g of the silica-R805/PMMA composites increases from 113 °C to 131 °C as the silica loading increases to 4 wt%, while that of the silica-R812/PMMA and silica-R972 increases from 113 °C to 126 °C and 125 °C, respectively. The adhesion between the particles and PMMA molecules is strong, so T_g of these composites increased with the polymer restriction of the chain by the modified silica particles and the dispersion of the silica particles in PMMA matrix. The tendency of T_g to vary with tan δ is consistent with that obtained from DSC.

3.2. Scan electron microscopy (SEM)

The most direct measurement of the dispersion of these silica particles in the PMMA matrix is made by SEM. Fig. 9 displays the SEM micrographs of the cross-sections of silica-R805/PMMA nanocomposites, and the silica particles dispersed in the PMMA matrix in the case of 1–4 wt% silica loading. The proportion of particles increased with the silica content, and the modified silica particles are well dispersed. The particles are sized between 70 nm and 110 nm. Fig. 10 displays two different modified silica/PMMA composites and unmodified silica/PMMA composites with 4 wt% loading. These silica particles dispersed locally in the polymer phase, and the individual silica particles started to form large aggregations. A comparison with Figs. 9 and 10 clearly indicates that silica-R805 particles can disperse effectively in the PMMA matrix, but other kinds of silica (R812, R972 and unmodified silica) begin to aggregate into large silica particles. Accordingly, increasing the number of hydrophobic groups on the surface of silica can prevent the aggregation of the silica

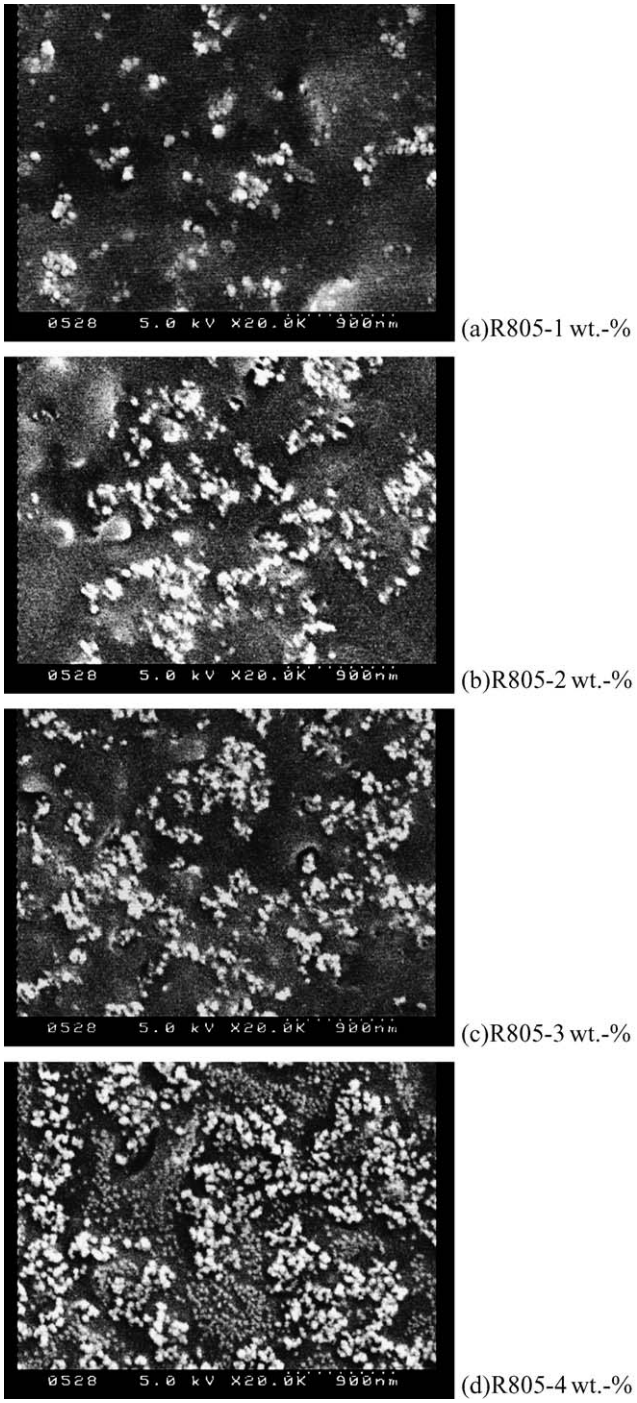

Fig. 9. SEM micrographs of silica-R805/PMMA nanocomposites with various silica contents: (a) 1 wt.-%, (b) 2 wt.-%, (c) 3 wt.-%, and (d) 4 wt.-%.

particles. The aggregation of the silica particles leads to poor properties of the silica/PMMA nanocomposites.

Briefly, the mechanical properties of these modified silica/PMMA nanocomposites are related to the interactions between the alkyl group on the silica surface and the PMMA matrix; the effective dispersion of inorganic fillers greatly increases the surface area of the modified silica. Therefore, the silica-R805/PMMA nanocomposites have

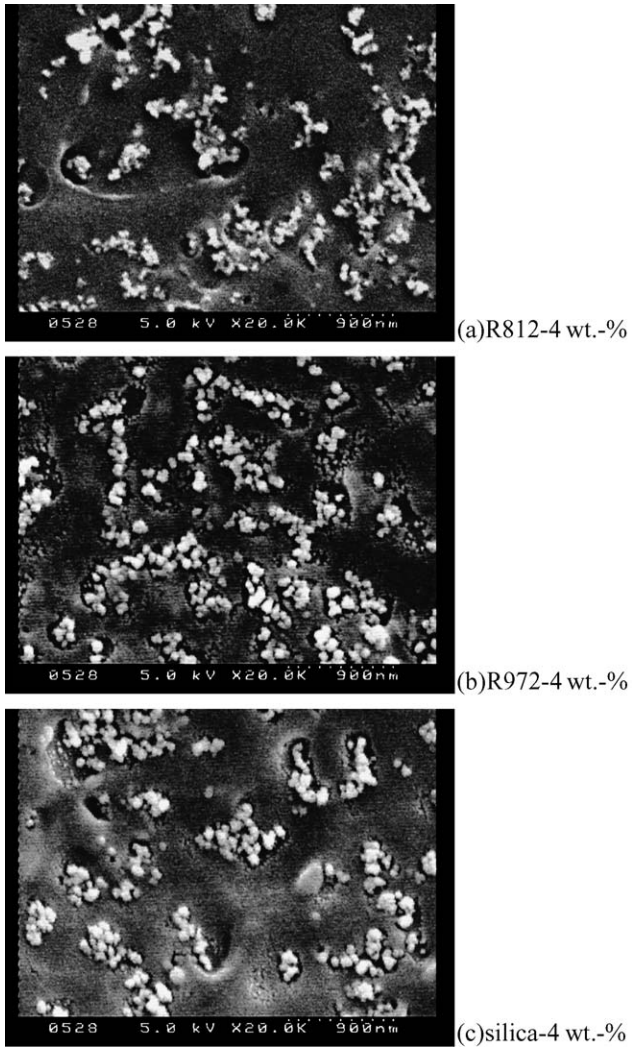

Fig. 10. SEM micrographs of different silica/PMMA nanocomposites with silica content 4 wt.-%: (a) silica-R812, (b) silica-R972, and (c) not modified silica.

a higher storage modulus and loss modulus than silica-R812/PMMA and silica-R972/PMMA.

3.3. Thermal properties of modified silica/PMMA nanocomposites

The thermal stability of silica/PMMA nanocomposites is governed by the modification of silica particles. Hence, the study of the thermal behaviors of silica particles is important. Fig. 11 shows the TGA weight loss and derivative thermograms (DTG) for organically modified silica in an atmosphere of nitrogen. The major differences between these organic silicas arise in the temperature range 400–600 °C—especially for silica-R805. The weight lost by the modified silica-R972 is very low between 50 °C and 600 °C. Any peaks in a derivative plot of this region reveal the presence of organic material. The organic constituent in organic

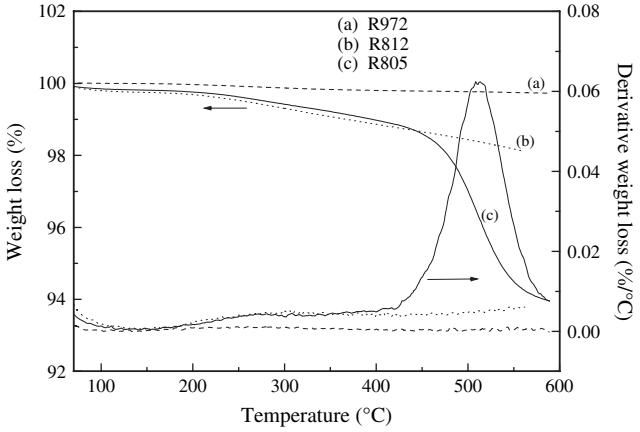

Fig. 11. The comparison of TGA and DTG curves for (a) silica-R972, (b) silica-R812, and (c) silica-R805.

silica-R805 starts to decompose at around 400 °C, and the maximum in the derivative curve is at 525 °C. Thus, the thermal stabilities of the modified silica are in the order R972 > R812 > R805.

Fig. 12 displays typical dynamic thermogravimetric TGA weight loss and derivative thermograms for variously modified silica/PMMA composites with 1 wt% added silica in a nitrogen environment. Pure PMMA decomposes in two stages: in the first stage, the weight loss gradually decreases as it is loaded with various organic silica composites. The thermal stability of pristine PMMA is related to the "weak links" in the radical-polymerized PMMA as the principal initiation sites of degradation [20–22]. The second steps in degradation of PMMA are attributed to the presence of head-to-head linkages, the lack of saturation of the end groups related to the combination and termination of two radicals and random scission. The degradation behaviors of these composites in an environment of nitrogen are dissimilar. Interestingly, silica-R972/PMMA nanocomposite is more thermally stable than the other modified silica/PMMA nanocomposites, but does not have the most favorable mechanical characteristics. The mechanical properties connect with the entanglements between the modified silica particles and the PMMA chain motion, while the thermal resistance is related to the thermal stability of modified silica particles and the polymer matrix. Therefore, the silica-R805/PMMA has the most favorable mechanical properties and the silica-R972/PMMA is the most thermally stable.

Aruchamy et al. [30] and Morgan et al. [31] also observed that unmodified silica/PMMA composites have higher decomposition temperatures than pure PMMA. Morgan et al. explained their results by the "trapping effect" of SiO_2 particles on the degradation products. Aruchamy and others [30,32–34] proposed that a hydrogen-bonding interaction between carbonyl groups in PMMA and Si–OH groups on silica surfaces may explain the improved stability. PMMA forms hydrogen bonds with silica; this H-bonding influences the electron density in pairs of polymer molecules. This explanation is unlikely to pertain in this investigation because the Si–OH group on the silica surface is unlikely to be present in the modified silica surface. The results indicate that the H-bonding might interrupt the depropagation of the chain. More interaction sites correspond to a higher decomposition temperature.

Fig. 13 plots the isothermal thermogravimetric curves for silica/PMMA nanocomposites variously modified at 220 °C for 2 h. The modified silica/PMMA composites decompose more slowly than the pure PMMA. Clearly, the silica-R972/PMMA composites have greater thermal resistance than other composites. The initial decomposition of the PMMA is accompanied by scission of the unsaturated end group. The silica particles in the polymer matrix trap the radicals and act as a gas barrier, preventing MMA monomers from permeating

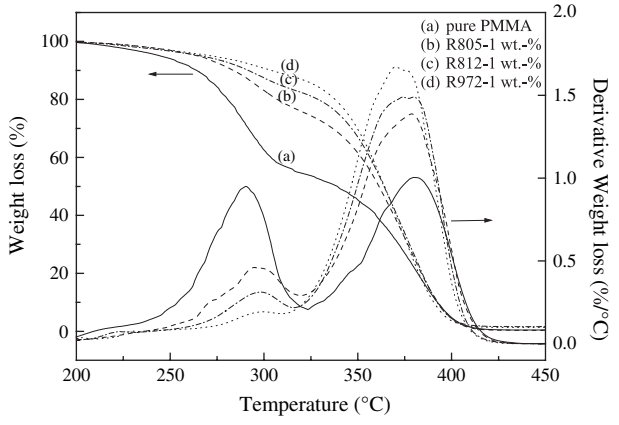

Fig. 12. The comparison of TGA and DTG curves for different silica/PMMA nanocomposites at heating rate 20 °C/min: (a) pure PMMA, (b) R805-1 wt.-%, (c) R812-1 wt.-%, and (d) R972-1 wt.-%.

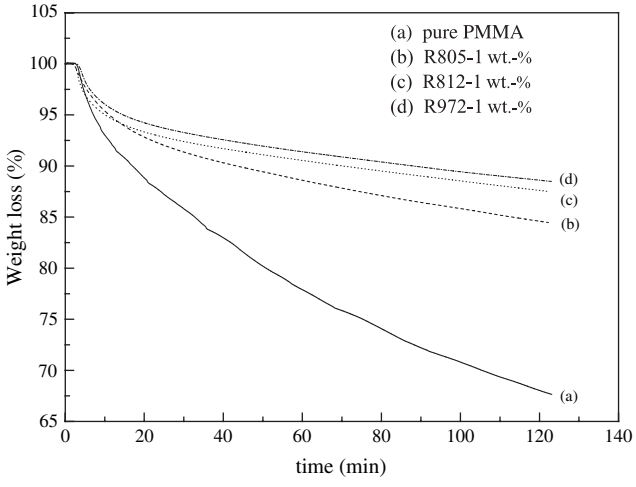

Fig. 13. Isothermal TGA curves of different silica/PMMA nanocomposites with 1 wt.-% content at 220 °C for 2 h.

out of the silica/PMMA composites during thermal treatment. Hence, the rate of decomposition of the silica/PMMA composites is lower than that of the pure PMMA.

Fig. 14 indicates the effect of modified silica content on the thermal decomposition temperature at 5% and 10% weight loss of the composites. The temperature of degradation at 10% weight loss is approximately 20–30 °C higher than that of pure PMMA. This result implies that a silica/PMMA nanocomposite is more thermally stable than pure PMMA. The effective dispersion of silica particles in the PMMA matrix enhances the thermal resistance of the silica/PMMA nanocomposites because increasing the number of active sites increases the decomposition temperature. Above 2 wt% silica loading, the decomposition temperature of these composites remains almost constant, perhaps because few silica particles are aggregated in the PMMA matrix. The rise in the decomposition temperature of the composites depends on both the dispersion behavior of the inorganic layers in the polymer matrix and the number of active sites in the silica particles that might trap radicals.

3.4. Thermal degradation kinetics

The activation energy (E_a) of degradation can be determined using the methods of Flynn [25–27], Kissinger [27–29] and Ozawa–Flynn [25,26,28].

Flynn proposed the use of the non-isothermal differential weight loss (DTGA) method at a constant heating rate β to evaluate the activation energy. This method is applied to estimate the initial degradation energy between 1 and 5%. Fig. 15 plots $T^2(dX/dT)$ versus the extent of conversion of PMMA with various modified silica/PMMA composites. The activation energies can be calculated from the slopes. Table 1 lists

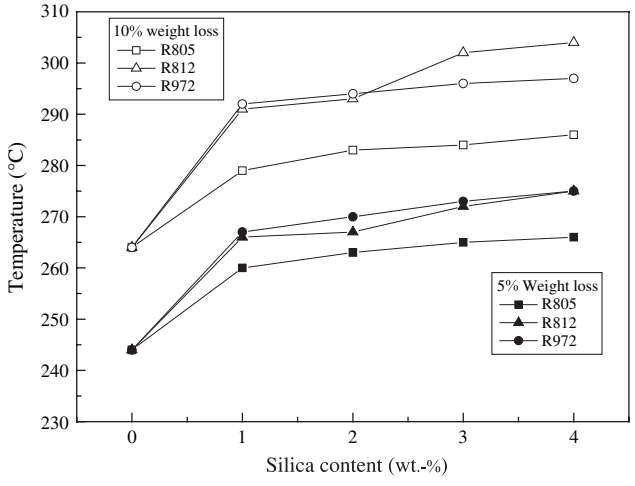

Fig. 14. Effect of silica content on the decomposition temperature at 5% and 10% weight loss of different silica/PMMA nanocomposites.

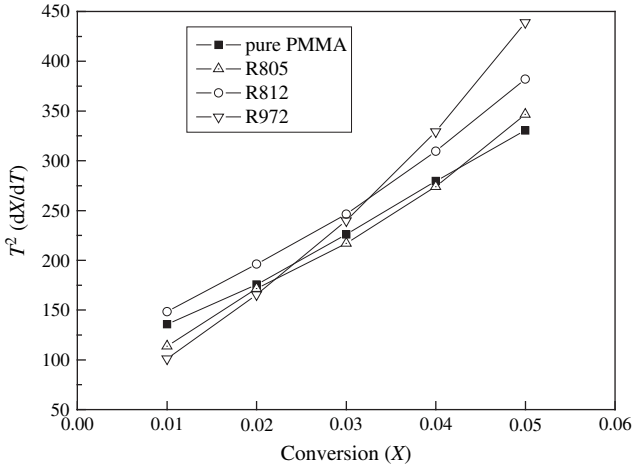

Fig. 15. The plot of $T^2(dX/dT)$ versus conversion (X).

the degradation activation energies of silica/PMMA composites with various silica contents. The activation energy of the silica/PMMA nanocomposites exceeds that of pure PMMA. This activation energy increases with the silica content. The pure PMMA has average activation energy 55 kJ/mol. Three modified silica nanocomposites, silica-R972/PMMA, silica-R812/PMMA and silica-R805/PMMA have activation energies in ranges 75–85 kJ/mol, 73–82 kJ/mol and 65–74 kJ/mol, respectively. Undoubtedly, the modified silica/PMMA nanocomposite has a higher thermal resistance than pure PMMA. The groups on the silica surface also affect the thermal behavior. As the number of alkyl group on the modified silica surface increased, the activation energy declined. Thus, the order of effects of the alkyl group on silica surface to the thermal stability of silica/PMMA composites can be concluded as R972 ~ R812 > R805.

The second method involves non-isothermal TGA measurement, developed by Kissinger at a constant rate of degradation, to evaluate the average decomposition energy at weight losses between 0 and 20%. A plot of $\ln[(dx/dT)/(1-x)]$ against $1/T$ yields a straight line that fits the data from the decomposition, the gradient of which provides the activation energy. Table 2 summarizes the experimental results. The silica/PMMA has a mean activation energy of above 96–126 kJ/mol for silica-R972/PMMA, 92–121 kJ/mol for silica-R812/

Table 1
The degradation activation energy (kJ/mol) of silica/PMMA nanocomposites measured by Flynn method (0–5% weight loss)

Silica content (wt.-%)	R972	R812	R805
0	55	55	55
1	75	73	65
2	81	72	72
3	79	78	73
4	88	82	75

Table 2
The degradation activation energy (kJ/mol) of silica/PMMA nanocomposites measured by Kissinger method (0–20% weight loss)

Silica content (wt.-%)	R972	R812	R805
0	72	72	72
1	96	92	85
2	112	110	88
3	125	120	90
4	126	121	99

PMMA and 85–99 kJ/mol for silica-R805/PMMA. The pure PMMA system has average activation energy of 72 kJ/mol. These results conclude that the silica/PMMA nanocomposite system has a higher activation energy and thermal resistance than pure PMMA. A comparison of the ranges of activation energies of the modified silica/PMMA nanocomposites reveals clearly that the thermal stability of the modified silica on PMMA follows the order, silica-R972/PMMA ~ -R812/PMMA > -R805/PMMA. The small aliphatic groups on the modified silica surface improve the thermal stability of PMMA. Thus, from the Kissinger analysis, it seems that the thermal stability of silica-R972/PMMA is slightly superior to silica-R812/PMMA composites, and both are much superior to silica-R805/PMMA.

The third method examines multiple heating rate kinetics (MHRK). The activation energies of degradation calculated from TG curves are based on mass losses in different decomposition regions during degradation process. Accordingly, a series of experiments were performed at various heating rates, and E_a was obtained from the slope of the linear isoconversion plot of ln (heating rate) against $1/T$. The lines in Fig. 16 are obtained for various conversions. The mean activation energies, summarized in Table 3, are determined from the slopes of the curves. The activation energies of 5, 10, 15 and 20% conversions of silica/PMMA are in the range 81–111 kJ/mol, while those of pristine PMMA are between 53 and 67 kJ/mol. The silica/PMMA nanocomposites are more thermally stable than pure PMMA. Furthermore, the aliphatic groups on the silica surface also affect the thermal resistance. The activation energy observably increased with percentage weight loss, and the thermal stabilities of the modified silica on PMMA follow the order silica-R972/PMMA ~ -R812/PMMA > -R805/PMMA.

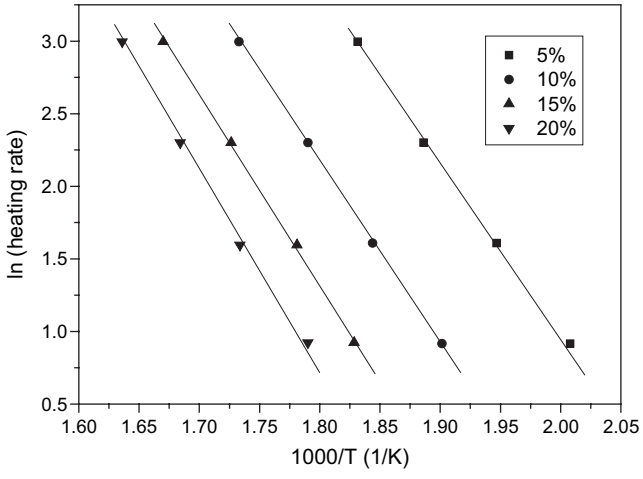

Fig. 16. The logarithm of heating rate versus temperature at constant conversion for the degradation of silica-R972/PMMA nanocomposites with 1 wt.-% loading.

Table 3
The degradation activation energy (kJ/mol) of silica/PMMA nanocomposites with 1 wt.-% loading measured by Ozawa and Flynn method

Weight loss %	Activation energy (kJ/mol)			
	Pure PMMA	R972	R812	R805
5	53	91	88	81
10	59	99	92	85
15	63	107	103	90
20	67	111	109	101

In summary, three methods were used to determine the thermal stability of silica/PMMA nanocomposites. Table 1 lists the activation energies of the initial degradation process (1–5% weight loss). The degradation proceeds as the temperature rises. Table 2 summarizes the activation energies of propagation (at 0–20% weight loss). Finally, the activation energies of certain conversions (5, 10, 15, and 20% weight loss) are determined by MHRK technique. These activation energies increase with percentage weight loss (Table 3). The results are similar for all nanocomposites. Incorporating a small amount of certain modified silica into the polymer matrix during the polymerization of MMA increased PMMA's thermal stability. As the length of the alkyl chain on the modified silica surface increased, the low-temperature end-scission of PMMA gradually decreased and the degradation temperature increased, implying that the large surface area of the silica and the higher thermal stability associated with inorganic fillers affected the thermal behavior.

4. Conclusion

This work considered three different specifics of modified silica particles in a PMMA matrix. Both the length of the alkyl chain on the modified silica surface and the dispersion behavior of these inorganic fillers affect the mechanical and thermal properties of the PMMA matrix. The silica-R805/PMMA nanocomposites have higher storage and loss moduli than both silica-R812/PMMA and silica-R972/PMMA. The degradation temperature and activation energy increased as the length of the alkyl chain on the modified silica

surface decreased. These results are attributed to the large silica surface area and fact that the silica particles might trap radicals during degradation.

Acknowledgements

The authors would like to thank the National Science Council of the Republic of China for financially supporting this research under Contract No. NSC90-2216-E006-026.

References

[1] Theng BKG. Formation and properties of clay–polymer complex. Amsterdam: Elsevier; 1979.
[2] Moet AS, Akelah A. Mater Lett 1993;18:97.
[3] Vaia RA, Ishii H, Giannelis EP. Chem Mater 1993;5:1694.
[4] Yano K, Usuki A, Okada A, Kurauchi T, Kamigaito O. J Poly Sci A 1993;31:2493.
[5] Lan T, Kaviratna PD, Pinnavaia TJ. Chem Mater 1994;6:573.
[6] Kojima Y, Usuki A, Kawasumi A, Okada A, Kurauchi T, Kamigaito O. J Poly Sci A 1993;31:983.
[7] Tien YI, Wei KH. Macromolecules 2001;34:9045.
[8] Tyan HL, Liu YC, Wei KH. Polymer 1999;40:4877.
[9] Ma Z, Kyotani T, Tomita A. Chem Commun 2000:2365.
[10] Yoon SB, Kim JY, Yu J. Chem Commun 2002:1536.
[11] Ryoo R, Joo SH, Jun S. J Phys Chem B 1999;103:7743.
[12] Wu CG, Bein T. Science 1994;266:1013.
[13] Yu JS, Kang S, Yoon SB, Chai G. J Am Chem Soc 2002;124:9382.
[14] Kang IK, Yoon SB, Yu JS, Kim DP. Chem Commun 2002:1670.
[15] Li Z, Jaroniec M. J Am Chem Soc 2001;123:9208.
[16] Grassie N, Melville HW. Faraday Soc Discuss 1947;2:378.
[17] Brockhaus A, Jenckel E. Makramol Chem 1956;19:262.
[18] Madorsky SL. J Polym Sci 1953;11:491.
[19] Hirata T, Kashiwagi T, Brown JE. Macromolecules 1985;18:1410.
[20] Kashiwagi T, Inaba A, Brown JE, Hatada K, Kitayama T, Masuda E. Macromolecules 1986;19:2160.
[21] Manring LE. Macromolecules 1988;21:528.
[22] Arisawa H, Brill TB. Combust Flame 1997;109:514.
[23] Bagby G, Lehrle RS, Robb JC. Polymer 1969;10:683.
[24] Holland BJ, Hay JN. Polymer 2001;42:4825.
[25] Flynn JH. In: Shalaby SW, editor. Thermal methods in polymer analysis. Philadelphia: The Franklin Institute Press; 1978.
[26] Chang WL. J Appl Polym Sci 1994;53:1759.
[27] Sanchez FH, Graziane RV. J Appl Polym Sci 1992;46:571.
[28] Ozawa T. Bull Chem Soc Jpn 1965;38:1881.
[29] Torf JCM, Deij L, Sorrepaal AJ, Heijens JC. Anal Chem 1984;56:2863.
[30] Aruchamy A, Blackmore KA, Zelinski BJJ, Uhlmanm DR, Booth C. Mater Res Soc Symp Proc 1992;249:353.
[31] Morgan AB, Antonucci JM, Vanlandingham MR, Harris RH, Kashiwagi T. Polym Mater Sci Eng 2000;83:57.
[32] Grohens Y, Brogly M, Labble C, Schultz J. Eur Polym J 1997;33:691.
[33] Thies C. J Polym Sci 1971;34:201.
[34] Dietz E. Makromol Chem 1976;177:2117.